Mechanical Engineering Faculty Research and Publications

Mechanical Engineering, Department of

4-2021

In situ TEM Characterization of Microstructure Evolution and Mechanical Behavior of the 3D-Printed Inconel 718 Exposed to High Temperature

Supriya Koul

Le Zhou

Omar Ahmed

Yongho Sohn

Tengfei Jiang

See next page for additional authors

Authors

Supriya Koul, Le Zhou, Omar Ahmed, Yongho Sohn, Tengfei Jiang, and Akihiro Kushima

Department of Mechanical Engineering Faculty Research and Publications/College of Engineering

In situ TEM Characterization of Microstructure Evolution and Mechanical Behavior of the 3D-Printed Inconel 718 Exposed to High Temperature

Supriya Koul
Department of Materials Science and Engineering, University of Central Florida, Orlando, FL, USA
Le Zhou
Department of Materials Science and Engineering, University of Central Florida, Orlando, FL, USA
Advanced Materials Processing and Analysis Center, University of Central Florida, Orlando, FL, USA
Department of Mechanical Engineering, Marquette University, Milwaukee, WI, USA
Omar Ahmed
Department of Materials Science and Engineering, University of Central Florida, Orlando, FL, USA
Yongho Sohn
Department of Materials Science and Engineering, University of Central Florida, Orlando, FL, USA

Advanced Materials Processing and Analysis Center, University of Central Florida, Orlando, FL, USA

Tengfei Jiang

Department of Materials Science and Engineering, University of Central Florida, Orlando, FL, USA
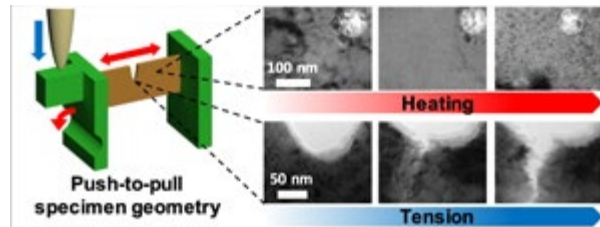
Akihiro Kushima

Department of Materials Science and Engineering, University of Central Florida, Olrando, FL, USA
Advanced Materials Processing and Analysis Center, University of Central Florida, Orlando, FL, USA
NanoScience Technology Center, University of Central Florida, Orlando, FL, USA

Abstract

This *in situ* transmission electron microscopy work presents a nanoscale characterization of the microstructural evolution in 3D-printed Inconel 718 (IN718) while exposed to elevated temperature and an associated change in the mechanical property under tensile loading. Here, we utilized a specially designed specimen shape that enables tensile testing of nano-sized thin films without off-plane deformations. Additionally, it allows a seamless transition from the *in situ* heating to tensile experiment using the same specimen, which enables a direct correlation of the microstructure and the mechanical property of the sample. The method was successfully used to observe the residual stress relaxation and the formation of incoherent γ' precipitates when temperature was increased to 700°C. The subsequent *in situ* tensile test revealed that the exposure of the as-printed IN718 to a high temperature without full heat treatment (solutionizing and double aging) leads to loss of ductility.

Keywords

additive manufacturing, heat treatment, in situ transmission electron microscopy, IN718, nanoscale mechanics

Introduction

Additive manufacturing (AM), commonly referred to as 3D printing, is expected to be a game-changer for the manufacturing industry (Aydinöz et al., Aydinöz, Brenne, Schaper, Schaak, Tillmann, Nellesen and Niendorf2016). The advancement of AM processes such as laser powder-bed fusion (LPBF) enables direct 3D printing of metal alloys. The LPBF method uses a scanning laser to melt or sinter (cohesive bonding) a powder-bed layer-by-layer to create complex and intricate three-dimensional geometries (Zhang et al., Zhang, Niu, Cao and Liu2015). This technology, compared to conventional manufacturing methods, has advantages such as design flexibility, thus evading the limiting factors such as production quantity, lead-time, and dimensions (Wang et al., Wang, Guan, Gao, Li, Chen and Zeng2012; Aydinöz et al., Aydinöz, Brenne, Schaper, Schaak, Tillmann, Nellesen and Niendorf2016; Trosch et al., Trosch, Strößner, Völkl and Glatzel2016; Kuo et al., Kuo, Horikawa and Kakehi2017*b*).

Several studies have been conducted to compare the mechanical properties of materials produced by LPBF and the traditional production methods involving casting and thermo-mechanical working (Wang et al., Wang, Guan, Gao, Li, Chen and Zeng2012; Zhang et al., Zhang, Niu, Cao and Liu2015; Trosch et al., Trosch, Strößner, Völkl and

Glatzel2016; Kuo et al., Kuo, Horikawa and Kakehi2017*a*). The distinct melting/solidification dynamics of LPBF is one of the biggest challenges in successfully implementing the AM technology. LPBF involves rapid heating and cooling, and together with the small laser spot size, it leads to the formation of nonequilibrium phases with characteristic microstructures (Kelly & Kampe, Kelly and Kampe2004; Mumtaz et al., Mumtaz, Erasenthiran and Hopkinson2008; Thijs et al., Thijs, Verhaeghe, Craeghs, Humbeeck and Kruth2010; Song et al., Song, Zhao, Li, Han, Wei, Wen, Liu and Shi2015; Li et al., Li, Li, Liu, Zhang, Zhou, Wei, Yan and Shi2016). Additionally, the microstructure of the LPBF-produced alloys can vary within the built sample (Baufeld et al., Baufeld, Biest and Gault2010; Thijs et al., Thijs, Van Humbeeck and Kruth2015) because of the variation in the cooling rate from the rapid cooling of the melt pool at the top part to the slow-cooled region at the lower part (or the region processed at the earlier stage). It is also highly dependent on the build direction. Columnar grains are commonly observed along the build direction in the LPBF alloys (Amato et al., Amato, Gaytan, Murr, Martinez, Shindo, Hernandez, Collins and Medina2012; Vilaro et al., Vilaro, Colin, Bartout, Nazé and Sennour2012; Mostafa et al., Mostafa, Picazo Rubio, Brailovski, Jahazi and Medraj2017) causing anisotropy in the mechanical properties (Zhao et al., Zhao, Chen, Lin and Huang2008; Frazier, Frazier2014; Song et al., Song, Zhao, Li, Han, Wei, Wen, Liu and Shi2015; Strößner et al., Strößner, Terock and Glatzel2015; Deev et al., Deev, Kuznetcov and Petrov2016). To achieve the desirable mechanical properties and thus meet the design specifications, the control of the microstructure by adequate solution heat treatment and aging is crucial (Zhou et al., Zhou, Mehta, McWilliams, Cho and Sohn2019). There are many parameters that affect the microstructure and, consequently, the mechanical properties of the LPBF-produced alloys. This includes, but is not limited to, laser power and spot sizes, scan speed and direction, hatch spacing, and slice thickness, to name a few. By changing these parameters, the microstructure and the mechanical properties can be altered even for the same alloy composition. And the postproduction heat treatment gives additional parameters leading to the fabrication of materials with a wide range of ductility and mechanical strengths (Ding et al., Ding, Muñiz-Lerma, Trask, Chou, Walker and Brochu2016). It is extremely challenging to optimize the entire processing route in order to achieve the target properties. Understanding the fundamental mechanism of the microstructure development and accompanying mechanical properties are essential for the efficient development of the LPBF processes. However, the knowledge and experience from conventionally manufactured alloys may not be directly applicable to LPBF alloys due to the difference in the microstructure.

There have been numerous studies comparing LPBF and the traditional production methods, such as casting and thermo-mechanical working (Wang et al., Wang, Guan, Gao, Li, Chen and Zeng2012; Zhang et al., Zhang, Niu, Cao and Liu2015; Trosch et al., Trosch, Strößner, Völkl and Glatzel2016; Kuo et al., Kuo, Horikawa and Kakehi2017*a*), and investigating the effect of the heat treatment on the microstructures and the mechanical properties of the LPBF alloys (Song et al., Song, Dong, Zhang, Liao and Coddet2012, Song, Dong, Liu, Liao and Coddet2014; Vrancken et al., Vrancken, Thijs, Kruth and Van Humbeeck2012; Chlebus et al., Chlebus, Gruber, Kuźnicka, Kurzac and Kurzynowski2015; Li et al., Li, Wang, Saunders, Suvorova, Zhang, Liu, Fang, Huang and Sercombe2015, Li, Li, Liu, Zhang, Zhou, Wei, Yan and Shi2016; Zhang et al., Zhang, Niu, Cao and Liu2015; Ter Haar et al., Ter Haar, Becker and Blaine2016; Tucho et al., Tucho, Cuvillier, Sjolyst-Kverneland and Hansen2017; Zhou et al., Zhou, Mehta, McWilliams, Cho and Sohn2019). Components manufactured using LPBF can achieve mechanical properties close to those of the conventional techniques or even better. However, mechanical properties of the as-printed alloys may not satisfy the requirement of the highly demanding applications because of their characteristic microstructures. For example, due to the rapid heating and cooling cycles of the LPBF process, solute partitioning is prevalent, leading to micro-segregation and subsequent formation of brittle intermetallics such as Laves phase (Tucho et al., Tucho, Cuvillier, Sjolyst-Kverneland and Hansen2017). Here, postproduction heat treatment is the key to enhancing the uniform elemental distribution and improving mechanical properties by promoting the precipitation of strengthening phases while eliminating the segregation

of undesired phases (Zhang et al., Zhang, Niu, Cao and Liu2015; Tucho et al., Tucho, Cuvillier, Sjolyst-Kverneland and Hansen2017).

Such postproduction heat-treatment studies have been well established for the bulk samples produced by conventional techniques, but limited information is available for powder-bed AM-processed samples (Zhang et al., Zhang, Yang, Song, Bai and Xiao2018; Sing et al., Sing, Huang and Yeong2020; Tsai et al., Tsai, Chen, Chao, Jang, Tsai, Su and Kuo2020). The LPBF-produced alloy may undergo a different structural evolution because its initial characteristic microstructure is different from those produced by the conventional routes. It is reported that during laser manufacturing of the IN718, the alloying elements, especially niobium (Nb) and molybdenum (Mo), tend to segregate in the inter-dendritic/cellular region compared to the conventionally produced alloys (Tucho et al., Tucho, Cuvillier, Sjolyst-Kverneland and Hansen2017). An enormous number of research works have been documented in the study of heat treatment and its relation to the deformation behavior in metallic structures. In the literature, several experimental and theoretical investigations account for analyzing the mechanical behavior of the bulk sample (de Formanoir et al., de Formanoir, Martin, Prima, Allain, Dessolier, Sun, Vivès, Hary, Bréchet and Godet2019; Hilaire et al., Hilaire, Andrieu and Wu2019; Sing et al., Sing, Huang and Yeong2020). Meanwhile, there are only a handful of studies on the LPBF-printed alloys at the submicron scale (Liu et al., Liu, Ding, Zhong, Zou, Wu, Chiu, Li, Zhang, Yu and Shen2018; Shen et al., Shen, Tian, Liu, Tang and Cheng2018; Bär et al., Bär, Berger, Jauer, Kurtuldu, Schäublin, Schleifenbaum and Löffler2019).

Since the LPBF alloy has unique microstructures that vary within the material, fine-scale analysis is necessary to fully understand their mechanical properties. Here, *in situ* transmission electron microscopy (TEM) and scanning electron microscopy (SEM) experiments have been widely used to capture the deformation and the fracture mechanics in the materials at nano- and atomic scales (Rao et al., Rao, Kumar, Srinivas and Sarma2003; Haque & Saif, Haque and Saif2004; Zhu & Espinosa, Zhu and Espinosa2005; Greer & Nix, Greer and Nix2006; Kiener & Minor, Kiener and Minor2011; Kushima et al., Kushima, Huang and Li2012; Imrich et al., Imrich, Kirchlechner, Kiener and Dehm2015; Wang et al., Wang, Zeng, Weinberger, Zhang, Zhu and Mao2015). For example, compressive tests of additively-manufactured micro-pillars with several microns of diameter can be performed inside an SEM to analyze the force–deformation responses (Daryadel et al., Daryadel, Behroozfar and Minary-Jolandan2019). Additionally, nanoindentation combined with SEM has been employed to study the mechanical properties of the LPBF-produced alloys and their spatial variations associated with the difference in the microstructures (Legros et al., Legros, Gianola and Motz2011). The technique allows the quantitative evaluation of the mechanical properties of the very fine micro-phases found in the LPBF.

On the other hand, *in situ* TEM provides direct observations of the intrinsic deformation mechanisms and their relationships with the microstructures at higher spatial resolutions. It allows the characterization of the nanostructures within the micro-phases and analysis of their effects on the mechanical properties through real-time observation of the dynamic processes during mechanical deformations. The *in situ* TEM techniques have been used to investigate structural changes in materials during heating (Liu et al., Liu, Yang and Ye2015; Wang & Haque, Wang and Haque2015; Rao et al., Rao, Diao, Ocelík, Vainchtein, Zhang, Kuo, Tang, Guo, Poplawsky, Zhou, Liaw and De Hosson2017; Callisti et al., Callisti, Tichelaar and Polcar2018; Topping et al., Topping, Ungár, Race, Harte, Garner, Baxter, Dumbill, Frankel and Preuss2018; Albu et al., Albu, Krisper, Lammer, Kothleitner, Fiocchi and Bassani2020) as well as deformation mechanisms at nano- and atomic scales (Haque & Saif, Haque and Saif2004; Zhu et al., Zhu, Moldovan and Espinosa2005; Kiener & Minor, Kiener and Minor2011; Wang et al., Wang, Zeng, Weinberger, Zhang, Zhu and Mao2015). Various *in situ* TEM mechanical testing methods were developed in the past decade, including nanocompression on focused ion beam (FIB) microfabricated pillars (Shan et al., Shan, Mishra, Syed Asif, Warren and Minor2008), bending tests using electric field-induced resonance (Wang et al., Wang, Kaplan-Ashiri, Wei, Rosentsveig, Wagner, Tenne and Peng2008), and microelectromechanical systems (MEMS) based on lithography for performing *in situ* TEM straining experiments

(Wang & Haque, Wang and Haque2015). MEMS fabrication technology of a freestanding tensile specimen with the force sensor and actuation mechanism for the force/displacement measurement shows distinct capabilities (Haque & Saif, Haque and Saif2004). The applications of these techniques have been explored with tremendous interest. For example, Minor et al. investigated the onset of plasticity using a miniature capacitive load–displacement transducer equipped on the TEM holder (Minor et al., Minor, Syed Asif, Shan, Stach, Cyrankowski, Wyrobek and Warren2006), and Liu et al. in their work revealed the effect of the dislocation network formed during selective laser melting on the dislocation motion by *in situ* TEM analysis using a straining holder (Liu et al. Liu, Ding, Zhong, Zou, Wu, Chiu, Li, Zhang, Yu and Shen2018).

These capabilities of the *in situ* TEM/SEM are important for establishing a fundamental understanding of the LPBF-produced alloys. In fact, several recent studies employed these techniques to study the AM process and the materials. The rapid solidification process of polycrystalline aluminum was observed by TEM using an ultrahigh frame-rate CCD camera with single-electron detection sensitivity (McKeown et al., McKeown, Zweiacker, Liu, Coughlin, Clarke, Baldwin, Gibbs, Roehling, Imhoff, Gibbs, Tourret, Wiezorek and Campbell2016; Zweiacker et al., Zweiacker, McKeown, Liu, LaGrange, Reed, Campbell and Wiezorek2016). Microstructure evolutions during the postprocess heating of the AM materials were investigated by *in situ* TEM for Ni-based superalloy (Deshpande et al., Deshpande, Deb Nath, Atre and Hsu2020), Ti-alloy (Li et al., Li, Jia, Yang, Liao, Jin, Cai and Zhou2021), and Al-alloy (Albu et al., Albu, Krisper, Lammer, Kothleitner, Fiocchi and Bassani2020). For the mechanical properties of AM-produced materials, the effect of the microstructure on the strength (Wu et al., Wu, Wang, Wang, Attallah and Loretto2016; Liu et al., Liu, Ding, Zhong, Zou, Wu, Chiu, Li, Zhang, Yu and Shen2018; Lin et al., Lin, Cao, Sokoluk, Jiang, Wang, Schoenung, Lavernia and Li2019) and fatigue behavior (Wang et al., Wang, Wu, Qian, Sun, Li and Correia2019) was studied by *in situ* TEM/SEM. However, performing *in situ* heating and mechanical tests on the exact same specimen to directly link the structural evolution and the mechanical property is still a challenging task.

Experimental Methodology

In this work, a unique *in situ* TEM procedure was developed to evaluate the microstructure evolution of LPBF-produced metal alloys when exposed to a high temperature and its effect on the mechanical property. This real-time experiment provides important insights regarding the evolution of the microstructure at different heating conditions and how the associated changes in the microstructures affect the mechanical properties. One of the biggest challenges during the *in situ* testing is maintaining the mechanical integrity because nanoscale samples are so thin. A significant amount of stress accumulates while thinning down using a FIB, which makes the sample intrinsically more fragile. This challenge is further complicated by leveling the thin testing sample onto the tensioning mechanism to ensure that the pure tension is applied to the sample. Otherwise, other forces such as torsion or bending may occur in addition to the tension. The fundamental principle is to measure the displacement of the tensile sample accurately (Zhu & Espinosa, Zhu and Espinosa2005). Additionally, even a slight misalignment in the specimen orientation and loading direction can result in unaccounted flexural stresses on the specimen (Haque & Saif, Haque and Saif2002). Therefore, in order to seamlessly observe the change in the microstructure during heating and to conduct the mechanical test on the exact same sample inside the TEM, we designed a push-to-pull TEM sample configuration as shown in Figure 1. With the two ribs at the ends of the thin center part, off-plane motions such as bending and twisting of the film are restricted. When a pushing force is applied on the protruding part on one of the ribs with the thinned root, the rib bends away from the support on the other side of the center lamella, and the pushing force is converted into the tensile load on the center of the specimen. Because the off-plane motions are constrained by the ribs, a tensile deformation of the observation area can be achieved without undesired bending and twisting. Here, a notch was introduced as a stress concentration site to nucleate a crack and initiate the fracture, since it is very difficult to observe a specific feature at high magnification (Wang & Haque, Wang and Haque2015). A finite element analysis was conducted

to confirm that the offset of the force does not affect the stress distribution at the crack tip (see Supplementary Material for details).
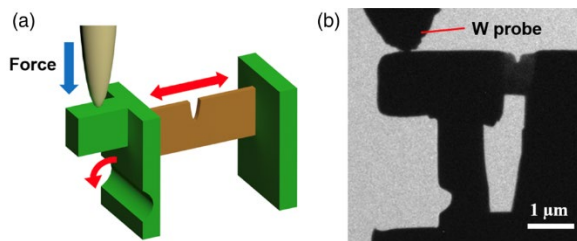

Fig. 1. (a) Schematic illustration of the push-to-pull sample configuration proposed in this work and (b) a TEM micrograph of the specimen prepared from scanning laser manufacturing-produced IN718.

A specimen block with dimensions of 5 μm × 2 μm × 2 μm was cut from a LPBF-produced alloy and shaped by FIB using a FEI 200 TEM FIB to the push-to-pull geometry as shown in Figure 1. The detailed procedure is explained in Supplementary Figure S4. FIB current was carefully controlled to minimize the beam damage that may affect the mechanical property of the specimen (Kiener et al., Kiener, Motz, Rester, Jenko and Dehm2007). The sample was heated inside the TEM using a heating holder (Gatan Model 652) for residual stress relaxation; the heated sample was then transferred to a 3D-nanomanipulation holder (Hummingbird Scientific) for tensile testing. A tungsten probe was used to apply the quasi-static displacement on the freestanding end of the FIB-prepared end of the specimen.

IN718 fabricated by LPBF was used as the subject of the study. The pre-alloyed IN718 gas-atomized powder with a diameter ranging from 10 to 45 μm was built into cubic samples by scanning laser manufacturing (SLM) 125HL LPBF unit. A laser beam of 200 W at a scanning speed of 900 mm/s in an argon atmosphere was used to fuse the powder particles. The details are recorded elsewhere (Zhou et al., Zhou, Mehta, McWilliams, Cho and Sohn2019). First, an *in situ* heating experiment was conducted to confirm that the microstructure evolution can be captured with our setup. A thin TEM specimen was prepared using FIB. The specimen was mounted on the *in situ* heating holder, and the temperature was raised inside the TEM to analyze the nucleation and the growth of precipitates (γ′, γ″). First, the temperature was increased from room temperature (~20°C) to 600°C at a heating rate of 50°C/min. The increase in temperature caused a sudden drift due to thermal expansion. After the drift was stabilized for 20 min, the temperature was raised to 700°C at a slower rate of 10°C/min.

Results and Discussion

Microstructural Evolution under Heating

Figure 2 shows the structural evolution of precipitates while heating (see also Supplementary Movie 1). The as-printed IN718 sample had a significant amount of residual stress due to fast heating/cooling processes in SLM. As the sample was heated, the stress was relieved (ii–iv) and the strain contrast was no longer visible at 640°C (iv). At 680°C, small precipitates began to nucleate in the matrix as indicated by the arrowheads (v). As the temperature increased, the precipitates continued to nucleate and grow introducing local strains in the material as shown in (vi). Electron diffraction patterns before and after the heating experiment were analyzed to confirm that the precipitates were γ′ and γ″ phases (see Supplementary Figs. 6 and 7). Furthermore, increasing the temperature to 800°C (at a rate of 10°C/min) resulted in the formation of a needle-like δ-phase (see Supplementary Fig. 5(d)). However, no Laves phases were found in our study, which agrees with Amato et al. (Amato, Gaytan, Murr, Martinez, Shindo, Hernandez, Collins and Medina2012). γ″ phase is metastable which transforms into δ-phase with similar composition and acicular structure at high temperature. This acicular δ-phase conversion reaction is accelerated around 800°C and would be highly undesirable because of the δ-phase

embrittlement. The amount of δ-phase that formed in the sample was comparatively low because the IN718 alloy studied in this work has Nb in the range of 4.75–5.50 wt%, while it should be more than 7% for significant distributions of δ-phase (Zhang et al., Zhang, Zhang, Cheng and Li2010; Kuo et al., Kuo, Horikawa and Kakehi2017*a*, Kuo, Horikawa and Kakehi2017*b*). The above observations indicate that the microstructure evolution of the IN718 at high temperature can be captured within a thin TEM specimen used in this work.
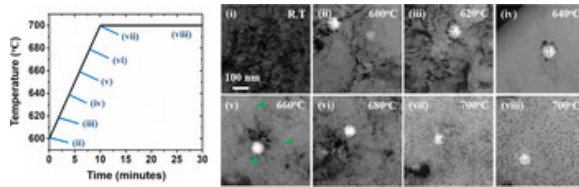

Fig. 2. Temperature change and the corresponding microstructure evolution of SLM-produced IN718 during *in situ* heating experiment. The sample morphology at room temperature before heating is shown in (i) as a reference. The residual stress in the as-produced sample was relaxed (ii, iii) and completely removed at 640°C (iv). At 660°C, precipitates started to nucleate as indicated by the arrowheads (v) accompanying local stresses as can be seen from the strain contrast. More precipitates nucleated and grew as the temperature was increased (vi, vii). When the sample was held at 700°C, the precipitates were uniformly distributed in the sample and the stress had been relaxed (viii).

Deformation and Fracture Behavior

To analyze the effect of the microstructure evolution on the mechanical properties, two specimens were cut from a single grain in as-printed IN718 within a few micrometers of each other and shaped into the push-to-pull samples as shown in Figure 1. Here, the tungsten probe was pushed against the sample at a displacement rate of 1.0 nm/s to apply tension to the thin observation area. Figure 3 shows the fracture process observed for the IN718 sample before heating (see also Supplementary Movies 3 and 4). Tensile deformation was successfully applied to the observation area, and the fracture process was captured. As the tension was applied to the specimen, the notch started to open wider (Figs. 3a and 3b). When further strain was imposed, a crack slowly nucleated from the surface as indicated by the arrowhead (Fig. 3c). Then, the crack started to open and propagated through the specimen (Figs. 3d–3f). At the latter stage of the deformation just before the fracture (Figs. 3g–3i), necking was observed, indicating a ductile fracture. After heating to 800°C in a same manner as described above (direct heating in TEM), the fracture process of the specimen showed completely different behavior as shown in Figure 4 (see also Supplementary Movies 5 and 6). A crack initiated from the notch at much smaller strain compared to the as-printed sample (Figs. 4a–4c). Once the crack was nucleated, it propagated rapidly across the specimen (Figs. 4d–4f) and led to the final fracture (Fig. 4g). The specimen showed no necking after the fracture (Fig. 4h), and the higher magnification images of the rough fracture surface indicated that the process was brittle.
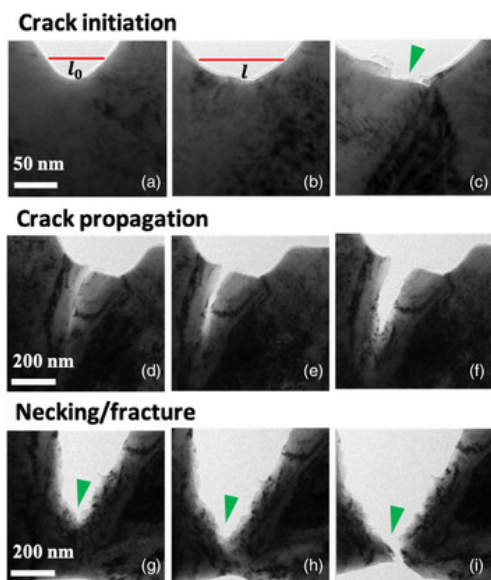
Fig. 3. Sequential TEM images of the fracture process of as-printed IN718: (a–c) crack initiation, (d–f) propagation, and (g–i) necking to ductile fracture.
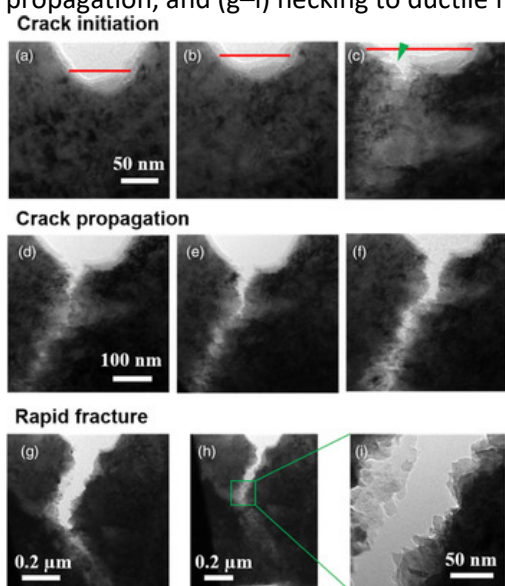

Fig. 4. Sequential TEM images of the fracture process of SLM-produced IN718 after exposure to elevated temperature inside TEM: (a–c) crack initiation, (d–f) propagation, and (g–i) rapid cleavage fracture.

As a comparison, a push-to-pull tensile specimen was cut from the "fully heat-treated" IN718 (Zhou et al., Zhou, Mehta, McWilliams, Cho and Sohn2019). It was solution heat-treated at 1,065°C for 1 h followed by the two-step aging at 720°C for 8 h and 650°C for 7 h, with γ'/γ'' precipitates coherent with the γ matrix. This sample, hereafter, is referred to as fully heat treated (FHT). As shown in Figure 5, the deformation behavior was different from the as-printed and directly heated specimen as discussed above. At the initiation stage, a network of nano-sized cracks was formed near the notch, forming 5–10 nm grains in the region marked by the dashed square (Fig. 5b). The detailed view of the crack nucleation site is shown in Supplementary Figure 8. The size of the grains matches well with the coherent γ' and γ'' precipitates. As the tension continued, the crack propagated rapidly (Figs. 5c–5e). However, it did not lead to a complete fracture as in the directly heated specimen. Instead, it showed necking before the fracture as indicated by the arrowheads (Figs. 5f–5h). These results demonstrate the important correlation between heat treatment, microstructural constituents (i.e., γ'/ γ'' precipitates and δ-phase), and mechanical properties (i.e., strength, ductility, and fracture toughness). To quantify the ductility of

the LPBF-produced IN718 before heating (i.e., as-built), after direct heating, and the proper two-stage heat treatment, the relationship between the crack length and the notch opening was analyzed. The initial notch size l_0 is indicated by the solid lines as shown in Figures 3a, 4a, and 5a. The features in the samples were tracked to determine the evolution of the notch size and the crack length. Figure 6 shows the relationship between the crack length and the notch opening, $\Delta l = l - l_0$. (Relationships between crack length, notch opening, and the displacement of the indentor are shown in Supplementary Fig. S9.) The crack developed slowly for the as-printed sample, and the length increased linearly as the notch opened. The directly heated sample showed a rapid increase in the crack length at a much smaller notch opening that corresponded to the brittle fracture. On the other hand, the crack length increased slowly for the FHT sample during its propagation, showing a ductile behavior. While both directly heated and FHT samples improved their strength due to the precipitation hardening, only the latter specimen with coherent precipitates maintained its toughness. Since the specimen was prepared from a single grain, the samples tested were single crystal. Therefore, the effect of needle-like δ-phase segregation at the grain boundary that restricts the dislocation motion (Trosch et al., Trosch, Strößner, Völkl and Glatzel2016; Kuo et al., Kuo, Horikawa and Kakehi2017*a*) was not present in the as-printed IN718 specimen. This enables dislocations to propagate freely and allows easy gliding of the crystallographic planes leading to the ductile deformation (see Supplementary Fig. S10). On the other hand, the abrupt fracture at the lower strain in the sample after direct heating to 800°C is attributed to the improper heat treatment, which caused a segregated formation of precipitates leading to several nucleation sites for catastrophic failure (Zhou et al., Zhou, Mehta, McWilliams, Cho and Sohn2019). Here, the embrittling precipitates formed in the specimen after heating causes dislocation pinning, which restricts the sliding of the crystallographic planes and causes brittle fracture. A similar ductile-to-brittle transition from the as-printed IN718 alloy after heating was reported for the bulk specimen (Popovich et al., Popovich, Borisov, Popovich, Sufiiarov, Masaylo and Alzina2017). The reason attributed to this behavior was the large amount of needle-like δ precipitates and undissolved Laves phases. Our observation demonstrated that the matrix grain itself also loses ductility as incoherent γ′/ γ″ phases precipitate.
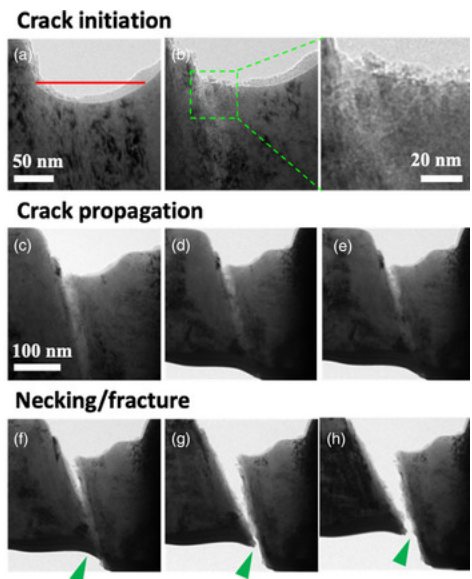

Fig. 5. Sequential TEM images of the fracture process of SLM-produced IN718 after solutionizing and aging: (a,b) crack initiation, (c–e) propagation, and (f–h) ductile fracture.
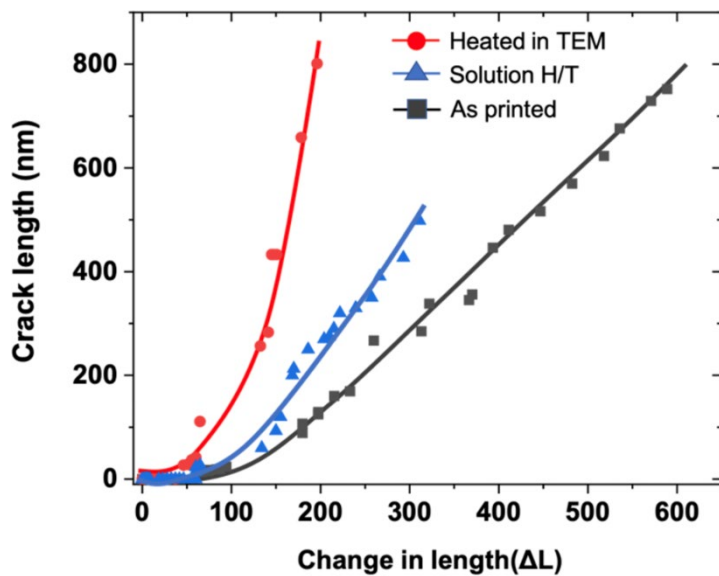
Fig. 6. Relationships between crack length and the notch opening of the IN718 specimen produced by SLM: as-printed (square), heated in TEM holder (circle), and solution heat treated (triangle).

Conclusion

Great attention has been paid to LPBF production and postproduction heat treatment parameters to produce desired microstructure and eliminate pores. Our observation confirms that as-printed IN718 is less suited for high-temperature applications, and that a simple postprint heating (e.g., direct heating) cannot ensure its mechanical properties. However, further improvements may be possible by tailoring the nanostructures within the grains. For example, the hardness of the LPBF-produced IN718 was improved by the precipitation of coherent γ' and γ'' precipitates following the full heat treatment (Zhang et al., Zhang, Zhang, Cheng and Li2010; Kuo et al., Kuo, Horikawa and Kakehi2017*b*; Zhou et al., Zhou, Mehta, McWilliams, Cho and Sohn2019). An effectively homogenizing solution treatment is necessary for subsequent precipitation hardening to properly take place while preventing the microsegregation of incoherent precipitates within the grains that lead to the embrittlement of LPBF-produced IN718. Although this work focused on LPBF-produced IN718 alloy and evaluated the relationships between microstructural evolution and the mechanical properties, the unique technique developed in this work is not restricted to the field of LPBF, but can be widely used to study the mechanical behavior of materials, including ceramics, biomaterials, and semiconductors, where the relationship among processing, nano/micro-structure, and mechanical properties elucidates the performance of engineered components and systems.

Supplementary material

To view supplementary material for this article, please visit https://doi.org/10.1017/S1431927621000052.

Acknowledgments

References

Albu, M, Krisper, R, Lammer, J, Kothleitner, G, Fiocchi, J & Bassani, P (2020). Microstructure evolution during in-situ heating of AlSi10Mg alloy powders and additive manufactured parts. Addit Manuf 36, 101605.

Amato, KN, Gaytan, SM, Murr, LE, Martinez, E, Shindo, PW, Hernandez, J, Collins, S & Medina, F (2012). Microstructures and mechanical behavior of Inconel 718 fabricated by selective laser melting. Acta Mater 60(5), 2229–2239.

Aydinöz, ME, Brenne, F, Schaper, M, Schaak, C, Tillmann, W, Nellesen, J & Niendorf, T (2016). On the microstructural and mechanical properties of post-treated additively manufactured Inconel 718 superalloy under quasi-static and cyclic loading. Mater Sci Eng A 669, 246–258.

Bär, F, Berger, L, Jauer, L, Kurtuldu, G, Schäublin, R, Schleifenbaum, JH & Löffler, JF (2019). Laser additive manufacturing of biodegradable magnesium alloy WE43: A detailed microstructure analysis. Acta Biomater 98, 36–49.

Baufeld, B, Biest, OVd & Gault, R (2010). Additive manufacturing of Ti–6Al–4 V components by shaped metal deposition: Microstructure and mechanical properties. Mater Des 31, S106–S111.

Callisti, M, Tichelaar, FD & Polcar, T (2018). In situ TEM observations on the structural evolution of a nanocrystalline W-Ti alloy at elevated temperatures. J Alloys Compd 749, 1000–1008.

Chlebus, E, Gruber, K, Kuźnicka, B, Kurzac, J & Kurzynowski, T (2015). Effect of heat treatment on the microstructure and mechanical properties of Inconel 718 processed by selective laser melting. Mater Sci Eng A 639, 647–655.

Daryadel, S, Behroozfar, A & Minary-Jolandan, M (2019). A microscale additive manufacturing approach for in situ nanomechanics. Mater Sci Eng A 767, 138441.

Deev, AA, Kuznetcov, PA & Petrov, SN (2016). Anisotropy of mechanical properties and its correlation with the structure of the stainless steel 316L produced by the SLM method. Phys Procedia 83, 789–796.

De Formanoir, C, Martin, G, Prima, F, Allain, SYP, Dessolier, T, Sun, F, Vivès, S, Hary, B, Bréchet, Y & Godet, S (2019). Micromechanical behavior and thermal stability of a dual-phase $\alpha+\alpha'$ titanium alloy produced by additive manufacturing. Acta Mater 162, 149–162.

Deshpande, A, Deb Nath, S, Atre, S & Hsu, K (2020). Effect of post processing heat treatment routes on microstructure and mechanical property evolution of Haynes 282 Ni-based superalloy fabricated with selective Laser melting (SLM). Metals 10(5), 629.

Ding, Y, Muñiz-Lerma, JA, Trask, M, Chou, S, Walker, A & Brochu, M (2016). Microstructure and mechanical property considerations in additive manufacturing of aluminum alloys. MRS Bull 41(10), 745–751.

Frazier, WE (2014). Metal additive manufacturing: A review. J Mater Eng Perform 23(6), 1917–1928.

Greer, JR & Nix, WD (2006). Nanoscale gold pillars strengthened through dislocation starvation. Phys Rev B 73(24), 245410.

Haque, MA & Saif, MTA (2002). In-situ tensile testing of nano-scale specimens in SEM and TEM. Exp Mech 42(1), 123–128.

Haque, MA & Saif, MTA (2004). Deformation mechanisms in free-standing nanoscale thin films: A quantitative in situ transmission electron microscope study. Proc Natl Acad Sci U S A 101(17), 6335–6340.

Hilaire, A, Andrieu, E & Wu, X (2019). High-temperature mechanical properties of alloy 718 produced by laser powder bed fusion with different processing parameters. Addit Manuf 26, 147–160.

Imrich, PJ, Kirchlechner, C, Kiener, D & Dehm, G (2015). Internal and external stresses: In situ TEM compression of Cu bicrystals containing a twin boundary. Scr Mater 100, 94–97.

Kelly, SM & Kampe, SL (2004). Microstructural evolution in laser-deposited multilayer Ti-6Al-4V builds: Part I. Microstructural characterization. Metall Mater Trans A 35(6), 1861–1867.

Kiener, D & Minor, AM (2011). Source truncation and exhaustion: Insights from quantitative in situ TEM tensile testing. Nano Lett 11(9), 3816–3820.

Kiener, D, Motz, C, Rester, M, Jenko, M & Dehm, G (2007). FIB damage of Cu and possible consequences for miniaturized mechanical tests. Mater Sci Eng A 459(1), 262–272.

Kuo, Y-L, Horikawa, S & Kakehi, K (2017 *a*). The effect of interdendritic δ phase on the mechanical properties of alloy 718 built up by additive manufacturing. Mater Des 116, 411–418.

Kuo, Y-L, Horikawa, S & Kakehi, K (2017 *b*). Effects of build direction and heat treatment on creep properties of Ni-base superalloy built up by additive manufacturing. Scr Mater 129, 74–78.

Kushima, A, Huang, JY & Li, J (2012). Quantitative fracture strength and plasticity measurements of lithiated silicon nanowires by in situ TEM tensile experiments. ACS Nano 6(11), 9425–9432.

Legros, M, Gianola, DS & Motz, C (2011). Quantitative in situ mechanical testing in electron microscopes. MRS Bull 35(5), 354–360.

Li, H, Jia, D, Yang, Z, Liao, X, Jin, H, Cai, D & Zhou, Y (2021). Effect of heat treatment on microstructure evolution and mechanical properties of selective laser melted Ti–6Al–4 V and TiB/Ti–6Al–4 V composite: A comparative study. Mater Sci Eng A 801, 140415.

Li, W, Li, S, Liu, J, Zhang, A, Zhou, Y, Wei, Q, Yan, C & Shi, Y (2016). Effect of heat treatment on AlSi10Mg alloy fabricated by selective laser melting: Microstructure evolution, mechanical properties and fracture mechanism. Mater Sci Eng A 663, 116–125.

Li, XP, Wang, XJ, Saunders, M, Suvorova, A, Zhang, LC, Liu, YJ, Fang, MH, Huang, ZH & Sercombe, TB (2015). A selective laser melting and solution heat treatment refined Al–12Si alloy with a controllable ultrafine eutectic microstructure and 25% tensile ductility. Acta Mater 95, 74–82.

Lin, T-C, Cao, C, Sokoluk, M, Jiang, L, Wang, X, Schoenung, JM, Lavernia, EJ & Li, X (2019). Aluminum with dispersed nanoparticles by laser additive manufacturing. Nat Commun 10(1), 4124.

Liu, JF, Yang, ZQ & Ye, HQ (2015). In situ transmission electron microscopy investigation of quasicrystal-crystal transformations in Mg–Zn–Y alloys. J Alloys Compd 621, 179–188.

Liu, L, Ding, Q, Zhong, Y, Zou, J, Wu, J, Chiu, Y-L, Li, J, Zhang, Z, Yu, Q & Shen, Z (2018). Dislocation network in additive manufactured steel breaks strength–ductility trade-off. Mater Today 21(4), 354–361.

McKeown, JT, Zweiacker, K, Liu, C, Coughlin, DR, Clarke, AJ, Baldwin, JK, Gibbs, JW, Roehling, JD, Imhoff, SD, Gibbs, PJ, Tourret, D, Wiezorek, JMK & Campbell, GH (2016). Time-resolved in situ measurements during rapid alloy solidification: Experimental insight for additive manufacturing. JOM 68(3), 985–999.

Minor, AM, Syed Asif, SA, Shan, Z, Stach, EA, Cyrankowski, E, Wyrobek, TJ & Warren, OL (2006). A new view of the onset of plasticity during the nanoindentation of aluminium. Nat Mater 5(9), 697–702.

Mostafa, A, Picazo Rubio, I, Brailovski, V, Jahazi, M & Medraj, M (2017). Structure, texture and phases in 3D printed IN718 alloy subjected to homogenization and HIP treatments. Metals 7(6), 196.

Mumtaz, KA, Erasenthiran, P & Hopkinson, N (2008). High density selective laser melting of Waspaloy®. J Mater Process Technol 195(1), 77–87.

Popovich, VA, Borisov, EV, Popovich, AA, Sufiiarov, VS, Masaylo, DV & Alzina, L (2017). Impact of heat treatment on mechanical behaviour of Inconel 718 processed with tailored microstructure by selective laser melting. Mater Des 131, 12–22.

Rao, GA, Kumar, M, Srinivas, M & Sarma, DS (2003). Effect of standard heat treatment on the microstructure and mechanical properties of hot isostatically pressed superalloy Inconel 718. Mater Sci Eng A 355(1), 114–125.

Rao, JC, Diao, HY, Ocelík, V, Vainchtein, D, Zhang, C, Kuo, C, Tang, Z, Guo, W, Poplawsky, JD, Zhou, Y, Liaw, PK & De Hosson, JTM (2017). Secondary phases in Al_xCoCrFeNi high-entropy alloys: An in-situ TEM heating study and thermodynamic appraisal. Acta Mater 131, 206–220.

Shan, ZW, Mishra, RK, Syed Asif, SA, Warren, OL & Minor, AM (2008). Mechanical annealing and source-limited deformation in submicrometre-diameter Ni crystals. Nat Mater 7(2), 115–119.

Shen, M-Y, Tian, X-J, Liu, D, Tang, H-B & Cheng, X (2018). Microstructure and fracture behavior of TiC particles reinforced Inconel 625 composites prepared by laser additive manufacturing. J Alloys Compd 734, 188–195.

Sing, SL, Huang, S & Yeong, WY (2020). Effect of solution heat treatment on microstructure and mechanical properties of laser powder bed fusion produced cobalt-28chromium-6molybdenum. Mater Sci Eng A 769, 138511.

Song, B, Dong, S, Liu, Q, Liao, H & Coddet, C (2014). Vacuum heat treatment of iron parts produced by selective laser melting: Microstructure, residual stress and tensile behavior. Mater Des 54, 727–733.

Song, B, Dong, S, Zhang, B, Liao, H & Coddet, C (2012). Effects of processing parameters on microstructure and mechanical property of selective laser melted Ti6Al4 V. Mater Des 35, 120–125.

Song, B, Zhao, X, Li, S, Han, C, Wei, Q, Wen, S, Liu, J & Shi, Y (2015). Differences in microstructure and properties between selective laser melting and traditional manufacturing for fabrication of metal parts: A review. Front Mech Eng 10(2), 111–125.

Strößner, J, Terock, M & Glatzel, U (2015). Mechanical and microstructural investigation of nickel-based superalloy IN718 manufactured by selective laser melting (SLM). Adv Eng Mater 17(8), 1099–1105.

Ter Haar, GM, Becker, TH & Blaine, DC (2016). Influence of heat treatments on the microstructure and tensile behaviour of selective laser melting-produced TI-6AL-4V parts. South African J Ind Eng 27, 174–183.

Thijs, L, Van Humbeeck, J & Kruth, JP (2015). Processing AlSi10Mg by selective laser melting: Parameter optimisation and material characterisation. Mater Sci Technol 31(8), 917–923.

Thijs, L, Verhaeghe, F, Craeghs, T, Humbeeck, JV & Kruth, J-P (2010). A study of the microstructural evolution during selective laser melting of Ti–6Al–4 V. Acta Mater 58(9), 3303–3312.

Topping, M, Ungár, T, Race, CP, Harte, A, Garner, A, Baxter, F, Dumbill, S, Frankel, P & Preuss, M (2018). Investigating the thermal stability of irradiation-induced damage in a zirconium alloy with novel in situ techniques. Acta Mater 145, 255–263.

Trosch, T, Strößner, J, Völkl, R & Glatzel, U (2016). Microstructure and mechanical properties of selective laser melted Inconel 718 compared to forging and casting. Mater Lett 164, 428–431.

Tsai, M-T, Chen, Y-W, Chao, C-Y, Jang, JSC, Tsai, C-C, Su, Y-L & Kuo, C-N (2020). Heat-treatment effects on mechanical properties and microstructure evolution of Ti-6Al-4V alloy fabricated by laser powder bed fusion. J Alloys Compd 816, 152615.

Tucho, WM, Cuvillier, P, Sjolyst-Kverneland, A & Hansen, V (2017). Microstructure and hardness studies of Inconel 718 manufactured by selective laser melting before and after solution heat treatment. Mater Sci Eng A 689, 220–232.

Vilaro, T, Colin, C, Bartout, JD, Nazé, L & Sennour, M (2012). Microstructural and mechanical approaches of the selective laser melting process applied to a nickel-base superalloy. Mater Sci Eng A 534, 446–451.

Vrancken, B, Thijs, L, Kruth, J-P & Van Humbeeck, J (2012). Heat treatment of Ti6Al4 V produced by selective laser melting: Microstructure and mechanical properties. J Alloys Compd 541, 177–185.

Wang, B & Haque, MA (2015). In situ microstructural control and mechanical testing inside the transmission electron microscope at elevated temperatures. JOM 67(8), 1713–1720.

Wang, J, Zeng, Z, Weinberger, CR, Zhang, Z, Zhu, T & Mao, SX (2015). In situ atomic-scale observation of twinning-dominated deformation in nanoscale body-centred cubic tungsten. Nat Mater 14, 594.

Wang, MS, Kaplan-Ashiri, I, Wei, XL, Rosentsveig, R, Wagner, HD, Tenne, R & Peng, LM (2008). In situ TEM measurements of the mechanical properties and behavior of WS2 nanotubes. Nano Res 1(1), 22.

Wang, Z, Guan, K, Gao, M, Li, X, Chen, X & Zeng, X (2012). The microstructure and mechanical properties of deposited-IN718 by selective laser melting. J Alloys Compd 513, 518–523.

Wang, Z, Wu, W, Qian, G, Sun, L, Li, X & Correia, JAFO (2019). In-situ SEM investigation on fatigue behaviors of additive manufactured Al-Si10-Mg alloy at elevated temperature. Eng Fract Mech 214, 149–163.

Wu, J, Wang, XQ, Wang, W, Attallah, MM & Loretto, MH (2016). Microstructure and strength of selectively laser melted AlSi10Mg. Acta Mater 117, 311–320.

Zhang, D, Niu, W, Cao, X & Liu, Z (2015). Effect of standard heat treatment on the microstructure and mechanical properties of selective laser melting manufactured Inconel 718 superalloy. Mater Sci Eng A 644, 32–40.

Zhang, HY, Zhang, SH, Cheng, M & Li, ZX (2010). Deformation characteristics of δ phase in the delta-processed Inconel 718 alloy. Mater Charact 61(1), 49–53.

Zhang, M, Yang, Y, Song, C, Bai, Y & Xiao, Z (2018). An investigation into the aging behavior of CoCrMo alloys fabricated by selective laser melting. J Alloys Compd 750, 878–886.

Zhao, X, Chen, J, Lin, X & Huang, W (2008). Study on microstructure and mechanical properties of laser rapid forming Inconel 718. Mater Sci Eng A 478(1), 119–124.

Zhou, L, Mehta, A, McWilliams, B, Cho, K & Sohn, Y (2019). Microstructure, precipitates and mechanical properties of powder bed fused Inconel 718 before and after heat treatment. J Mater Sci Technol 35(6), 1153–1164.

Zhu, Y & Espinosa, HD (2005). An electromechanical material testing system for in situ electron microscopy and applications. Proc Natl Acad Sci U S A 102(41), 14503–14508.

Zhu, Y, Moldovan, N & Espinosa, HD (2005). A microelectromechanical load sensor for in situ electron and x-ray microscopy tensile testing of nanostructures. Appl Phys Lett 86(1), 013506.

Zweiacker, K, McKeown, JT, Liu, C, LaGrange, T, Reed, BW, Campbell, GH & Wiezorek, JMK (2016). Determination of crystal growth rates during rapid solidification of polycrystalline aluminum by nano-scale spatio-temporal resolution in situ transmission electron microscopy. J Appl Phys 120(5), 055106.